

# Extracellular potentials generated by axonal projections are shaped by patterns of bifurcations and terminations

Thomas McColgan, Hermann Wagner, Richard Kempter

September 4, 2015

## Introduction

Extracellular field potentials (EFPs) in the brain were long thought to be primarily synaptic in origin (Buzsáki et al., 2012). However, a number of recent data analysis and modeling studies have revealed that active, non-synaptic membrane currents can play a role in generating EFPs (Reimann et al., 2013).

The study of the fields is relevant in many measurement methods which rely on the extracellular field potential. The relevance may also including noninvasive methods, where the underlying mechanisms of far field generation are often poorly understood (Rattay and Danner, 2014).

- Make a distinction here between somatic EAPs and axonal EAPs. Reference recent and older work on somatodendritic EAPs.

The aim of this study is to understand how the EFP is influenced by the anatomical structure of the axons. In particular, we explain how typical projection patterns in which an axon bundle widens and then terminates in its projection area affect the EFP.

Such axon bundles exist throughout the peripheral and central nervous system. (Examples...) The white matter of the brain can be viewed as an agglomeration of such bundles. (ref)

It has been shown (Kuokkanen et al., 2010), that with sufficient spatial and temporal organization extracellular fields of axonal and synaptic sources can reach strengths on the order of several mV. Here we extend this finding to include more general axon bundles, including those receiving input with less temporal precision.

We characterize three principal effects of axon bundle structure on the EFP. These effects are elaborations of the properties of such bundles described in past (Plonsey, 1977; Gydikov and Trayanova, 1986; Gydikov et al., 1986). We find that the low-frequency components of the EFP are governed by the local density of bifurcations and terminations. The high-frequency components are governed by the local fiber density. Furthermore we show that the low-frequency components exceed the high-frequency components in spatial reach.

We demonstrate these properties using two models of varying complexity, both of them based on a forward model of the extracellular field potential (Holt and Koch, 1999; Gold et al., 2006). The first model includes a detailed multicompartiment model of the axon population. The second is an

analytically tractable simplification of the axon bundle. Finally, we demonstrate the properties in real data using as a set of in-vivo electrophysiological recordings from the barn owl brain stem.

- cite: rall, Rinzel, einevoll, Destexhe, Brette, nunez&srinivasan, telenzuk
- Some more refs to add: Denker et al 2011 Schomburg et al 2011 Ray Maunsell 2011, Belluscio 2012)

## Results

- Axonal projections generate a dipole-like field potential (**Fig 1A**)
  - long range
  - low frequency
  - Examples of phenomenology from literature
- General results for axonal projections :
  - The low-frequency (eg population rate pulse) parts are governed by the local density of bifurcations and terminations(**Fig 1B**)
  - The high-frequency (eg individual spikes, ‘noise’, neurophonic) parts are governed by the local fiber density(**Fig 1C**)
  - The low-frequency component exceeds the high-frequency component in reach (**Fig 2**)
- The barn owl neurophonic as an example that shows these properties(**Fig 3**)
  - The high-frequency component shows a steady increase in latency along the projections’ depth, while the low-frequency can have stationary parts caused by sharp increases or decreases of fiber number (bifurcations or terminations).
  - These aspects are reflected in the model
- Ways of understanding the effect
  - Single AP along single axon(**Fig 4**)
  - Analytical model(**Fig 5**)

## Discussion

- Relevance of Findings
  - Interpretation of CSD
    - \* Classical CSD: constant fiber density, variable currents
    - \* Here: variable fiber density, constant currents
  - Dipole has far field, ABR response?
- Compare to other auditory systems (Chicken NL, MSO)
  - Speculate on functional relevance of polarity shift (a la Rinzel & Goldwyn)
- compare to other fiber bundle systems

## Methods

- Experimental Methods
- Multicompartment Model
- Analytical Model

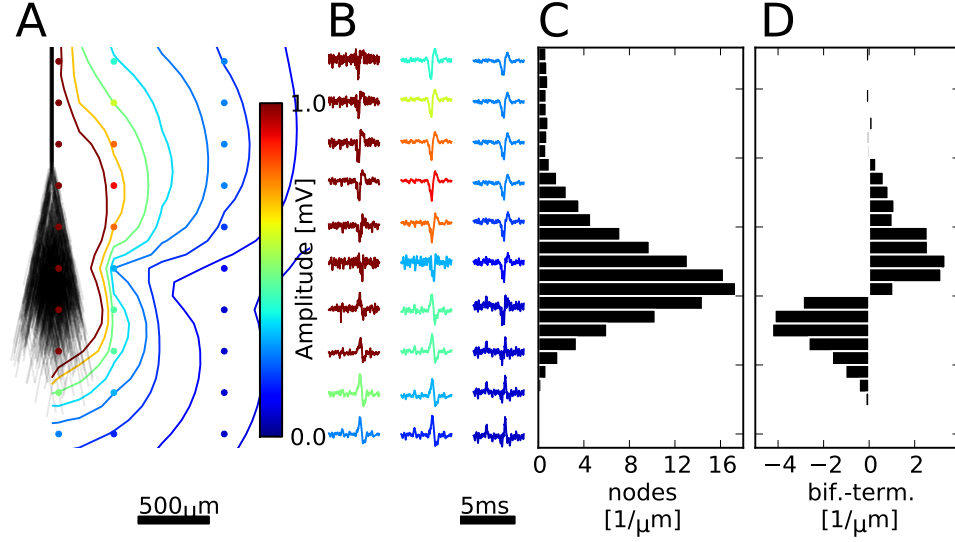


Figure 1: Axonal projections generate a dipole-like extracellular field potential. Extracellular evoked potential due to a pulse of activity in a generic fiber bundle. (A) shows the structure of the bundle, next to (B) EFP responses at various locations, indicated by colored dots. Scaling of traces indicated by colorbar. Relative strength of high-frequency noise relative to the low-frequency pulse decays with distance. The low frequency pulse switches polarity along the nerve bundles termination zone. (C) shows the fiber density overlayed with the strength of the high-frequency EFP component. (D) shows the density of bifurcations and terminations at varying depths.

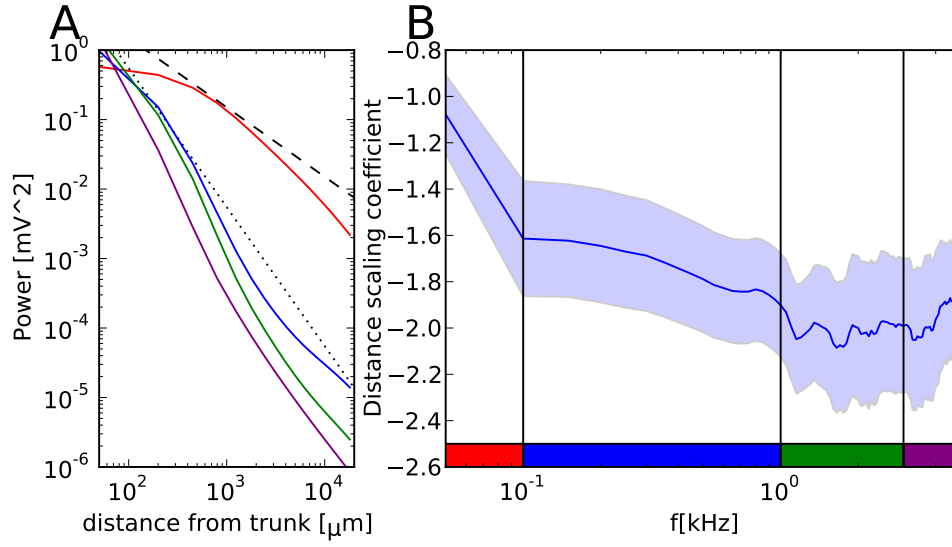


Figure 2: Low-frequency component of the axon bundle EFP exceeds high frequency in reach. (A) shows the behaviour of different spectral components (frequency indicated by colorbar) in a double logarithmic plot. The slope indicates the scaling coefficient in this frequency band. (B) shows this scaling coefficient for different frequencies. Low frequencies have the least negative coefficient, indicating the furthest reach.

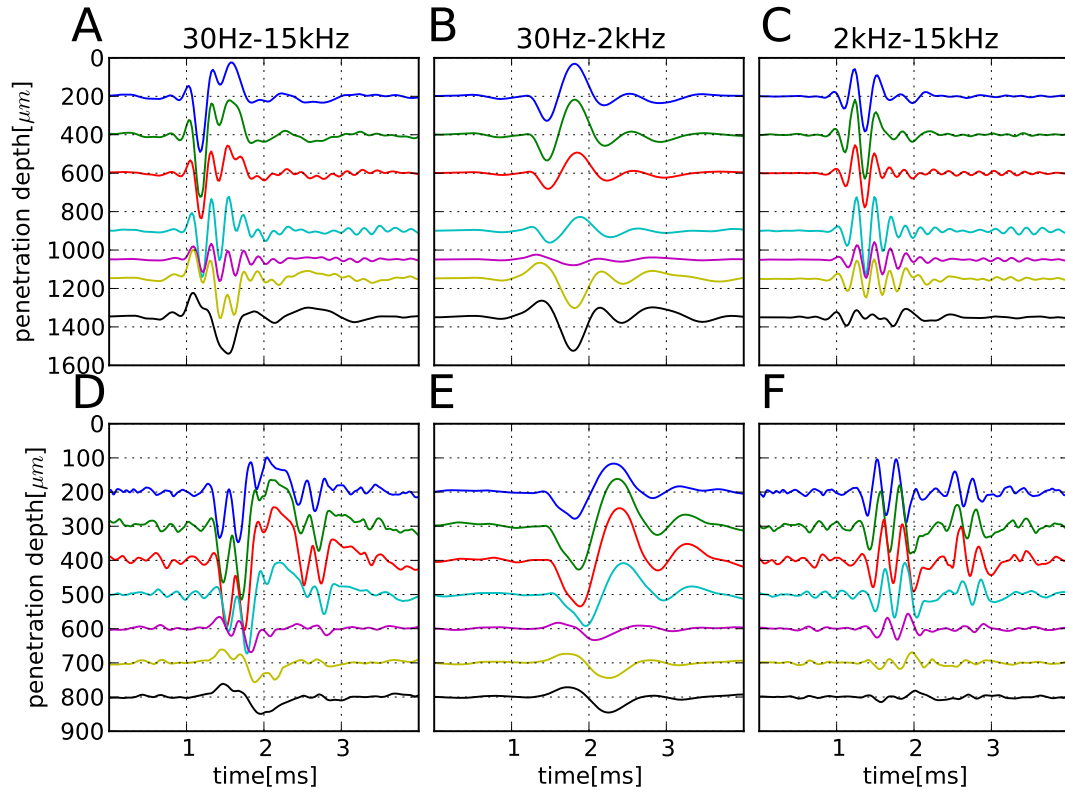


Figure 3: Data from the barn owl shows the expected behaviour predicted by the model. (**A-C**) shows data from the barn owls nucleus laminaris in response to an auditory click stimulus, compared to a simulation of the axonal structure and activation in (**D-F**). The click stimulus induces a pulse of activity in the afferent axon bundle. The low-frequency components (**B** and **E**) show the polarity reversal. The high frequency component (**C** and **F**), does not show such a reversal, but rather shows a steady increase in phase with depth.

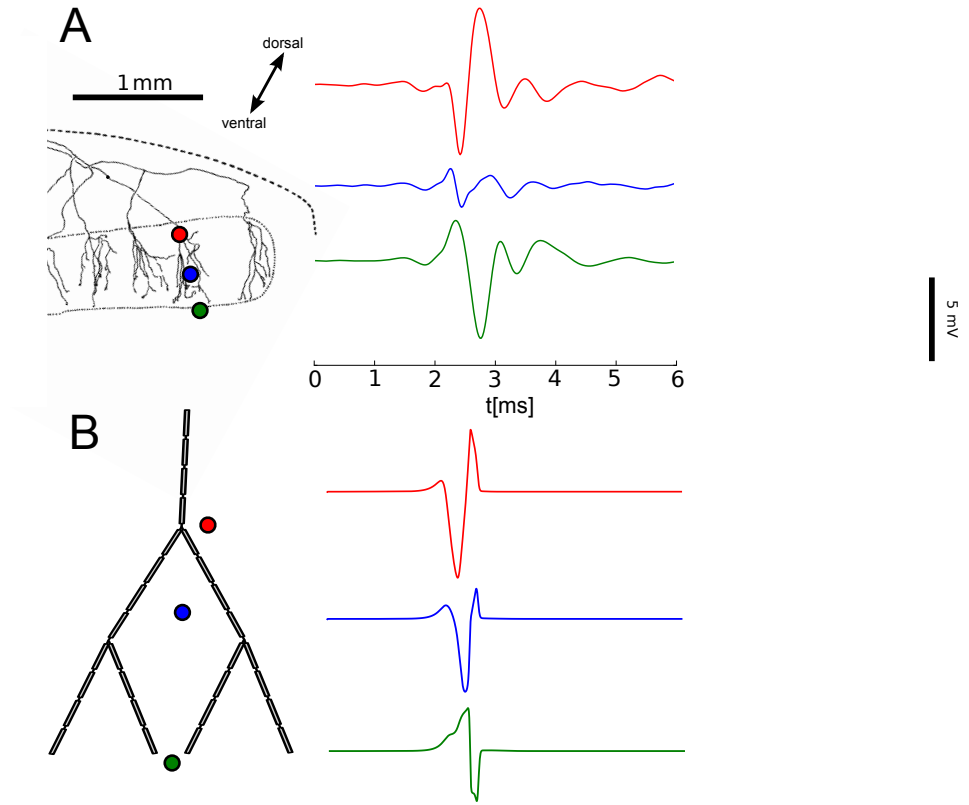


Figure 4: The dipolar behaviour can be understood by examining individual action potentials on a single axon tree. Comparing the low frequency owl data (**A**) to a single axon and action potential in model (**B**) shows a similar behaviour. In particular, the potential at a termination and that at a bifurcation (red and green curves in **B**) are approximately inverted.

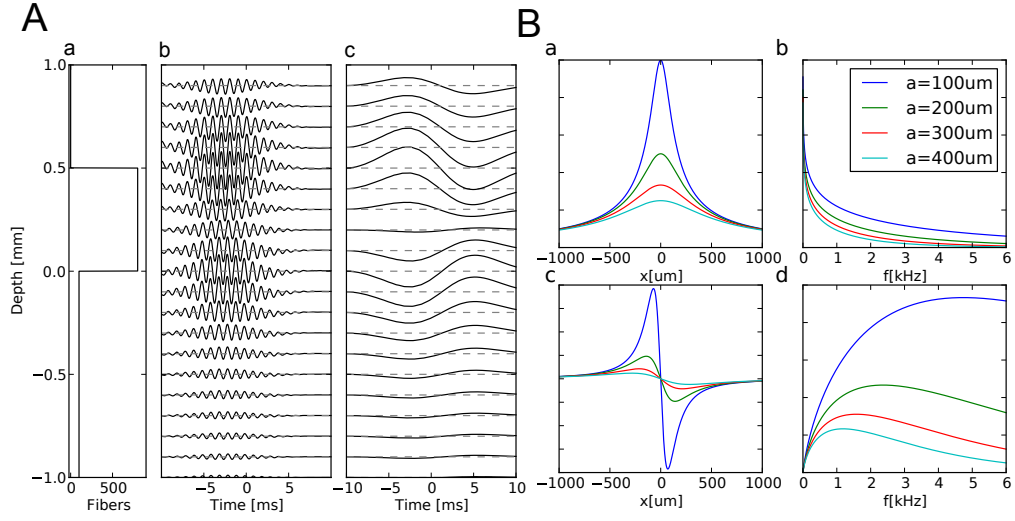


Figure 5: Analytical model of the axon bundle potential explains the effects observed in the numerical model and example data. **(A)** shows the behaviour of a simplified fiber bundle with a piecewise constant fiber density (**Aa**). The high frequency component (**Ab**) shows no polarity reversal, while the high-frequency component (**Ac**) does, as expected from the data and modelling. This can be understood by decomposing the signal into two components. The first component is governed by the bifurcation and termination density, and is filtered by the regular weighting function (**Ba**), which acts as a low-pass filter (**Bb**). The second component is governed by the fiber density, and is filtered by the derivative of the weighting function (**Bc**), which acts as a high- or band-pass filter (**Bd**).

## Bibliophraphy

Buzsáki G, Anastassiou CA, Koch C (2012) The origin of extracellular fields and currents — EEG, ECoG, LFP and spikes. *Nature Reviews Neuroscience* 13:407–420 Available at: <http://dx.doi.org/10.1038/nrn3241>.

Gold C, Henze DA, Koch C, Buzsáki G (2006) On the origin of the extracellular action potential waveform: A modeling study. *Journal of neurophysiology* 95:3113–3128 Available at: <http://dx.doi.org/10.1152/jn.00979.2005>.

Gydikov A, Gerilovsky L, Radicheva N, Trayanova N (1986) Influence of the muscle fibre end geometry on the extracellular potentials. 54:1–8 Available at: <http://dx.doi.org/10.1007/bf00337110>.

Gydikov AA, Trayanova NA (1986) Extracellular potentials of single active muscle fibres: Effects of finite fibre length. 53:363–372 Available at: <http://dx.doi.org/10.1007/bf00318202>.

Holt GR, Koch C (1999) Electrical Interactions via the Extracellular Potential Near Cell Bodies. *Journal of Computational Neuroscience* 6:169–184 Available at: <http://dx.doi.org/10.1023/a:1008832702585>.

Kuokkanen PT, Wagner H, Ashida G, Carr CE, Kempter R (2010) On the origin of the extracellular field potential in the nucleus laminaris of the barn owl (*Tyto alba*). *Journal of neurophysiology* 104:2274–2290 Available at: <http://dx.doi.org/10.1152/jn.00395.2010>.

Plonsey R (1977) Action potential sources and their volume conductor fields. *Proceedings of the IEEE* 65:601–611 Available at: <http://dx.doi.org/10.1109/proc.1977.10539>.

Rattay F, Danner SM (2014) Peak I of the human auditory brainstem response results from the somatic regions of type I spiral ganglion cells: Evidence from computer modeling. *Hearing research* 315C:67–79 Available at: <http://view.ncbi.nlm.nih.gov/pubmed/25019355>.

Reimann MW, Anastassiou CA, Perin R, Hill SL, Markram H, Koch C (2013) A Biophysically Detailed Model of Neocortical Local Field Potentials Predicts the Critical Role of Active Membrane Currents. *Neuron* 79:375–390 Available at: <http://dx.doi.org/10.1016/j.neuron.2013.05.023>.